Applied Surface Science 436 (2018) 527–535

Contents lists available at ScienceDirect

Applied Surface Science

journal homepage: www.elsevier.com/locate/apsusc

Full Length Article

Constructing superhydrophobic WO3@TiO2 nanoflake surface beyond amorphous alloy against electrochemical corrosion on iron steel

S.Q. Yu [a], Y.H. Ling [a,*], R.G. Wang [b], J. Zhang [a], F. Qin [a], Z.J. Zhang [a]

[a] Lab of Advanced Materials, School of Materials Sciences and Engineering, Tsinghua University, Beijing, 100084, China
[b] Department of Mechanical Systems Engineering, Faculty of Engineering, Hiroshima Institute of Technology, 2-1-1 Miyake, Saeki-ku, Hiroshima, 731-5193, Japan

ARTICLE INFO

Article history:
Received 17 September 2017
Received in revised form 7 November 2017
Accepted 25 November 2017
Available online 2 December 2017

Keywords:
Corrosion resistance
Superhydrophobicity
Photo-induced cathodic protection
WO_3@TiO_2
Nano-flake
Dealloying

ABSTRACT

To eliminate harmful localized corrosion, a new approach by constructing superhydrophobic WO_3@TiO_2 hierarchical nanoflake surface beyond FeW amorphous alloy formed on stainless steel was proposed. Facile dealloying and liquid deposition was employed at low temperature to form a nanostructured layer composing inner WO_3 nanoflakes coated with TiO_2 nanoparticles (NPs) layer. After further deposition of PFDS on nanoflakes, the contact angle reached 162° while the corrosion potential showed a negative shift of 230 mV under illumination, resulting in high corrosion resistance in 3.5 wt% NaCl solution. The tradeoff between superhydrophobic surface and photo-electro response was investigated. It was found that this surface feature makes 316 SS be immune to localized corrosion and a pronounced photo-induced process of electron storage/release as well as the stability of the functional layer were detected with or without illumination, and the mechanism behind this may be related to the increase of surface potential due to water repellence and the delayed cathodic protection of semiconducting coating derived mainly from the valence state changes of WO_3. This study demonstrates a simple and low-cost electrochemical approach for protection of steel and novel means to produce superhydrophobic surface and cathodic protection with controllable electron storage/release on engineering scale.

1. Introduction

Steel is widely utilized in modern society but one in ten of the metal productions around the world each year are junked due to corrosion [1]. How to reduce the economic loss and risk in application is still a big challenge. According to different corrosion mechanism, varieties of methods have been applied for metal corrosion inhibition, such as anticorrosion coatings [2–4], and cathodic protection [5]. However, material and energy loss usually occur in these methods. Therefore, an environment friendly and durable strategy with less input of energy and material loss is highly desired.

Electrochemical corrosion is always originated from the inherent micro/macro electrochemical inhomogeneities of steel in combination with environment factors, interruption between metal and surrounding environment interaction is therefore an effective method for corrosion inhibition [6]. Recently, superhydrophobic surface has aroused much interest due to its remarkable applications in fog-harvesting [7], oil-water separation [8], anti-icing [9] and self-cleaning [10–13]. With extraordinary water-repellent performance, superhydrophobic surface exhibits promising application for corrosion resistance and self-cleaning on steel [14–17]. Byungrak et al. [18] synthesized superhydrophobic surfaces on stainless steel via etching and oxidation processes for enhancing corrosion resistance but the contact angle decreased from 157.9° to 131.7° over one week. Zhang et al. [19] reported durable anticorrosion superhydrophobic surfaces on aluminum substrates through electrodeposition approach. Although the resulting surfaces remain superhydrophobic in 3.5 wt.% NaCl aqueous solution for 70 h, the contact angle decreased to 142.6 ± 4.8° in an abrasion test after being dragged to move on 1000 grit SiC emery paper under a pressure of 1.3 kPa in one direction for 600 mm. Therefore, taking consideration of the instability of the superhydrophobic surface, it is of vital importance to endow stainless steel with multiple protections [20]. And hydrophobicity needs to be enhanced and the mechanism on hydrophobic degradation waits to be further elucidated.

The essence in electrochemical corrosion is electron loss in anodic metals. As a result, cathodic protection logically becomes

* Corresponding author.
E-mail address: yhling@mail.tsinghua.edu.cn (Y.H. Ling).

https://doi.org/10.1016/j.apsusc.2017.11.211
0169-4332/

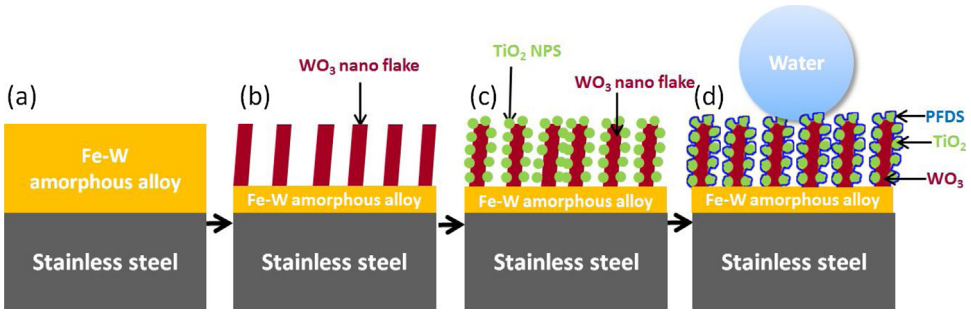

Fig. 1. Schematic illustration of the fabrication process of superhydrophobic WO_3@TiO_2 nanocomposite film via (a) codeposition of FeW alloy, (b) dealloying of iron, (c) liquid phase deposition of TiO_2 and (d) vapor deposition of PFDS.

the fundamental way to suppress corrosion. To efficiently reduce the electrical energy input and cost, the application of photo-induced cathodic protection on metallic material has been highly focused in recent researches since Tsujikawa et al. [21] revealed cathodic corrosion protection of TiO_2 on stainless steel under UV illumination [22–25]. However, its actual photo-induced cathodic protection is limited by three main factors: wide band gap (3.2 eV), recombination of photo-generated electron-hole pairs and no photo-generated electrons in dark for cathodic protection [26–28]. The combination of TiO_2 with other semiconductors (WO_3 [29], CdS [30], CdSe [31], SnO_2 [32,33], Ag_2S [34], and MoO_3 [35]) is an alternative strategy to settle these limitations, among which WO_3 is most promising for it has narrow bandgap energy of 2.6 eV which can be motivated under visible light illumination. And WO_3 exhibits electron storage ability that stores electrons under illumination and transports those electrons to the stainless steel once light is off [36]. Besides, the band structure of WO_3 matches that of TiO_2 so that charge transfer process can be facilitated [37]. Shen et al. [38] demonstrated good photo-oxidation efficiencies by WO_3@TiO_2 at elevated temperatures. Dozzi et al. [39] coupled TiO_2 with different amounts of WO_3 as photocatalysts and inhibited recombination of photo-generated electron-hole pairs. To acquire a higher quantum effect, WO_3@TiO_2 nanostructure is favorable. Momeni et al. [40] fabricated silver-loaded TiO_2-WO_3 nanotubes film as photo catalyst by electrochemical method. Hunge et al. [41] prepared stratified WO_3@TiO_2 thin film with 3D sheeted porous structure of TiO_2 on WO_3 as photoelectrochemical catalyst. Unfortunately, few of these structures involve TiO_2 nanoparticle decorated WO_3 nanoflake array skeleton. Besides, the interface incompatibility between semiconductor and metallic substrate construct great difficulties in practical application.

In this study, we tactfully constructed superhydrophobic surface on stainless steel using TiO_2 nanoparticles decorated WO_3 nanoflake arrays to combine photo-induced cathodic protection with superhydrophobicity, endowing stainless steel with double protection. The hierarchical nanostructured layer composing inner WO_3 nanoflakes and outer TiO_2 nanoparticles layer is synthesized on stainless steel via a novel and facile route involving electrodeposition and dealloying of FeW amorphous alloy, liquid-phase deposition of TiO_2 and subsequently annealing in air. The remaining precursor FeW amorphous alloy on 316 SS after dealloying has a disordered atomic-scale structure with no grain boundary and stacking defects, which has the potential to prevent localized corrosion such as pitting and stress cracking corrosion. Furthermore, continuous composition changes from 316 SS to FeW alloy and to WO_3 nanoflake arrays inhibit interface problem. Synergistic effects of superhydrophobicity and photo-induced cathodic protection on corrosion resistance of this WO_3@TiO_2 nanoflake arrays were analyzed in detail. Variations of open circuit potential, tafel curves and electrochemical impedance spectra of the film in 3.5 wt% NaCl were measured to evaluate the corrosion resistance of the surface.

2. Experimental

2.1. Nanostructures construction

The process for WO_3@TiO_2 nanocomposite structure fabrication is presented in Fig. 1(a). 316SS, the target material, was polished with #800, #1000, #1500, and #2000 abrasive papers and ultrasonically cleaned in acetone, deionized water and alcohol, respectively. (I) The first step was the electrodeposition of FeW amorphous alloy on stainless steel. A two-electrode system with the above 316 SS as cathode and graphite paper as the anode was designed, using an electrolyte containing 10.50 g $C_6H_8O_7{\cdot}H_2O$, 1.39 g $FeSO_4{\cdot}7H_2O$, 16.49 g $Na_2WO_4{\cdot}2H_2O$ and 100 mL H_2O. All chemicals were of analytical purity and were used without any further purification. Electrodepositing was conducted in a 60 °C water bath with 0.03 A/cm^2 current density for 90 s. (II) The second step was the formation of H_2WO_4 nanoflake arrays via dealloying by immersing FeW amorphous alloy coated specimen in 3.5 wt% HNO_3 for 20 h. (III) The third step was the fabrication of WO_3@TiO_2 nanoflake arrays. Liquid phase deposition was carried out by dipping the as-prepared nanoflakes film in the mixture of 10 mL 0.1 M $(NH_4)_2TiF_6$ and 10 mL0.6 M H_3BO_4 for 3.5 h. After that, the samples were subjected to heat-treatment at 400–600 °C in air. (IV) The as-prepared WO_3@TiO_2 nanocomposite film was modified with 1H, 1H, 2H, 2H, -Perfluorodecyltriethoxysilane ($C_{16}H_{19}F_{17}O_3Si$), (PFDS) liquid in a beaker sealed with Al foil and heated at 150 °C for 30 min [42].

2.2. Characterization and electrochemical measurement

The morphology of the film at different stages and crystallinity of the WO_3@TiO_2 composite film were characterized by FE-SEM (JEOL JSM-7001F) at 20 kV and FE-TEM (JEM-2100F) at 200 kV respectively. The phase composition was analyzed by Raman spectroscopy (Renishaw RM2000, 100–2000 nm) and X-ray diffraction (D/max-2500, Cu K_a radiation). The contact angle of the surface was measured using a video based contact angle measuring device (Dataphysics OCA15Pro). AFM (NTEGRA solaris, NT-MDT) was applied to measure the surface electronic work function and the probe used was SCM-PIT. Chemical state of the surface was analyzed by XPS (ULVAC-PHI, Quantro SXM). C1s peak of adventitious hydrocarbon at 284.60 eV was used to adjust all spectra and Shirley-type background removal was also applied. Composition of PFDS was characterized by FT-IR spectra (NETZSCH X70).

All electrochemical measurements were carried out in a three-electrode cell in 3.5 wt% NaCl aqueous solution, where the as-prepared samples acted as working electrode, a saturated calomel electrode acted as reference electrode, and platinum foil acted